

Will the Proliferation of 5G Base Stations Increase the Radio-Frequency Pollution?

Luca Chiaraviglio,^{1,2} Giuseppe Bianchi,^{1,2} Nicola Blefari-Melazzi,^{1,2} Marco Fiore,³

(1) Department of Electronic Engineering,

University of Rome Tor Vergata, Rome, Italy, email {luca.chiaraviglio,giuseppe.bianchi,blefari}@uniroma2.it

(2) Consorzio Nazionale Interuniversitario per le Telecomunicazioni, Italy

(3) Institute of Electronics, Computer and Telecommunication Engineering,

National Research Council of Italy, Turin, Italy, email marco.fiore@ieiit.cnr.it

Abstract—A common concern among the population is that installing new 5G Base Stations (BSs) over a given portion of territory results into an uncontrollable increase of Radio-Frequency (RF) pollution. To face this dispute in a way that is explainable also to a layman, we develop a very simple model, which evaluates the RF pollution at selected distances between the user and the 5G BS locations, e.g., at an average distance or at a fixed one. We then obtain closed-form expressions to quantify the RF pollution increase/decrease when comparing a pair of 5G deployments. Our results show that a dense 5G deployment is in general beneficial to the users living in proximity to the 5G BSs, with an abrupt decrease of RF pollution (up to three orders of magnitude) compared to a sparse deployment. However, we also show that, when a minimum sensitivity threshold is increased, the RF pollution from 5G BSs may be (lightly) increased.

Index Terms—5G Cellular Networks; Radio-Frequency Pollution; Base Station Deployment; Cell Densification

I. INTRODUCTION

5G is the dominant technology that is going to revolutionize the services provided through cellular networks in the coming years [1]. Clearly, in order to support the variegated services offered by this technology, new 5G Base Stations (BSs) have to be installed over the territory. In this context, a common opinion among the population is that living in proximity to a 5G BS is dangerous for health [2]. Although previous works in the literature have not shown any evidence of health effects triggered by living in proximity to radio BSs operating below maximum exposure limits (see e.g., [3], [4]), the debate about the installation of new 5G BSs is currently a hot topic, with several municipalities that are even denying the authorizations to install 5G BSs [5], on the basis of a precautionary principle.

In this scenario, the concern that 5G will bring an uncontrolled proliferation of 5G BSs and consequently of Radio-Frequency (RF) pollution clearly emerges. However, is this anxiety corroborated by scientific evidence? Even if the scientific community well knows that this is not the case, to the best of our knowledge, no previous papers have tackled the impact of 5G BSs proliferation in terms of RF pollution by adopting models understandable also by non technical readers. To shed light on this aspect, we introduce a set of simplifying (but worst case) assumptions, which lead us to derive a very

simple model that evaluates the RF pollution generated by a set of candidate 5G network deployments. We focus on regular BS coverage layouts, in which the coverage area of each BS is modeled with a regular shape (e.g. highway, square, hexagonal). Actually, such deployments are meaningful in dense population areas, like urban canyons and shopping malls, where the selection of BS sites is mainly driven by capacity constraints. We then link together the coverage layout, the operating frequency, the radiated power, the minimum sensitivity threshold, the level of RF pollution introduced by neighboring BSs and the channel propagation parameters. In this way, we obtain closed form expressions of RF pollution in terms of power received by a user at selected distances from the serving BS (e.g., at an average distance or a fixed one). By comparing the outcomes of different deployment types in a set of meaningful scenarios, we are able to assess the variation of 5G BSs RF pollution, due to the adoption of one deployment w.r.t. another one. Our results indicate that the RF pollution tends to promptly decrease at the selected locations when the number of 5G BSs is increased. Moreover, the RF pollution level from neighboring BSs does not significantly impact the outcomes. Eventually, we show that, under specific circumstances (e.g., when the minimum sensitivity threshold is increased), there may be a (light) increase of RF pollution from 5G BSs.

Previous works in the literature cover other aspects related to 5G deployments, e.g., in terms of 5G techno-economic assessment [6], joint power and ElectroMagnetic Fields (EMF) reduction [7], 5G planning under EMF limits [8]. We believe that all these aspects are surely of interest, but pretty orthogonal w.r.t. our work, which is instead tailored to the RF pollution assessment of 5G deployments.

The rest of the paper is organized as follows. Sec. II details the system model. Sec. III describes the scenarios. Sec. IV presents the results. Finally, Sec. V summarizes our outcomes and sketches future research activities.

II. SYSTEM MODEL

In this work, we consider the deployment of a set of 5G BSs to cover a set of pixels. Our analysis leverages on some standard topological/regularity/propagation assumptions,

namely: i) the BSs are placed on a regular layout, as we consider a dense deployment with a uniform distribution of users; consequently, each BS serves a portion of the total territory under consideration, ii) the BSs are characterized by common features in terms of coverage shape, coverage size, and adopted frequency; i.e., the same BS equipment is used across the set; iii) the propagation conditions are the same among the BSs in the set; e.g., the coverage distance is below the maximum value triggering a change in the path loss exponent [9].

Key Assumptions. We then introduce the following key assumptions, namely: i) the BS radiation pattern is omnidirectional, ii) the power of the BS is set to ensure a minimum sensitivity at the BS coverage edge, and iii) the level of RF pollution coming from the neighbor BSs is evaluated at the BS edge. In the following, we provide more details about why these assumptions are meaningful for our scopes.

Focusing on the first assumption, a real 5G BS generally exhibits a radiation pattern different than a omnidirectional one, because: i) sectorization is in general exploited, and ii) the extensive adoption of beamforming allows to concentrate the power on specific locations. With sectorization, the radiation patterns match the positioning of the sectors. With beamforming, the actual level of power that is received over the territory generally varies both in time and space, and it is normally estimated through statistical models [10]. Assuming an omnidirectional radiation is actually a worst case scenario, in which: i) each pixel is served by a beam (in other words: the beams are activated simultaneously in all the directions), ii) each pixel is not affected by sectorization (i.e., the received power is not decreased when the pixel is located at the sector edge). Therefore, this assumption leads to an over-estimation of the received RF pollution, thus corroborating the presented results.

The second assumption is about the setting of the BS power. Let us denote with \mathcal{I} and \mathcal{P} the set of 5G BSs and the set of pixels, respectively. $P_{(i)}^E$ is the power radiated by BS $i \in \mathcal{I}$ to cover the pixels in its coverage area. P_{TH}^R is the minimum power that has to be received by a pixel from a 5G BS providing 5G coverage. For every pixel $p \in \mathcal{P}$ in the coverage area of BS i , a minimum sensitivity threshold has to be ensured through the following constraint:

$$\frac{P_{(i)}^E}{d_{(p,i)}^\gamma \cdot f^\eta \cdot c} \geq P_{\text{TH}}^R \quad (1)$$

where $d_{(p,i)}$ is the distance between pixel p and 5G BS i , γ is the path loss exponent for the distance, f is the operating frequency, η is the path loss exponent for the frequency, and c is a baseline path loss. Since we consider a regular layout and a uniform user distribution, all the BSs belonging to the set radiate the same power, i.e., $P_{(i)}^E = P^E$. In addition, it is trivial to note that constraint (1) can be satisfied by setting P^E as:

$$P^E = P_{\text{TH}}^R \cdot d_{\text{MAX}}^\gamma \cdot f^\eta \cdot c \quad (2)$$

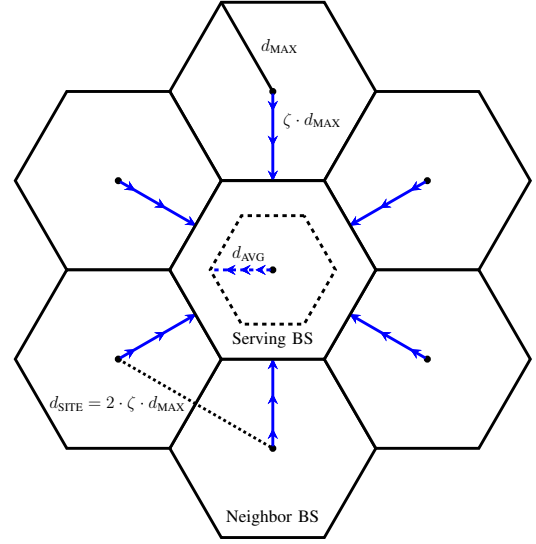


Fig. 1. Graphical sketch of the distances appearing in the RF pollution computation of Eq. (5). The RF pollution of the serving BS is evaluated at d_{AVG} . The RF pollution level from neighboring BSs is evaluated at $\zeta \cdot d_{\text{MAX}}$.

where d_{MAX} is the maximum coverage distance of a 5G BS. In other words, the received power at the BS edge is our reference to setup the BS power. In this scenario, the effect of interference from neighboring BSs and the impact of noise can be easily compensated by varying the values of P_{TH}^R .

The third assumption involves the RF pollution computation from the serving BS $s \in \mathcal{I}$ and the neighboring ones $i \in \mathcal{I}^{\text{NEIGH}}$, $i \neq s$, where $\mathcal{I}^{\text{NEIGH}} \subset \mathcal{I}$ is the subset of neighboring BS whose RF pollution can be sensed at pixel p . In general, the RF pollution $P_{(p)}^R$ that is received by a given pixel p is expressed as:

$$P_{(p)}^R = \underbrace{\frac{P^E}{d_{(p,s)}^\gamma \cdot f^\eta \cdot c}}_{\text{RF Pollution from serving BS}} + \sum_{i \in \mathcal{I}^{\text{NEIGH}}} \underbrace{\frac{P^E}{d_{(p,i)}^\gamma \cdot f^\eta \cdot c}}_{\text{RF pollution from neighbor BSs}} \quad (3)$$

Let us introduce the inter-site distance $d_{\text{SITE}} = 2 \cdot \zeta \cdot d_{\text{MAX}}$, where $\zeta \in (0, 1)$ is a parameter set in order to avoid coverage holes. We then assume that the RF pollution of the neighbors is evaluated at distance $d_{\text{SITE}}/2 = \zeta \cdot d_{\text{MAX}}$ for all neighbors $N^I = |\mathcal{I}^{\text{NEIGH}}|$. It is easy to note that this assumption leads to an Upper Bound (UB) of $P_{(p)}^R$ if $d_{(p,s)} \leq \zeta \cdot d_{\text{MAX}}$, where $d_{(p,s)}$ is the distance between pixel p and serving BS s . More formally, we have:

$$P_{(p)}^R \leq \underbrace{\frac{P^E}{d_{(p,s)}^\gamma \cdot f^\eta \cdot c}}_{\text{RF Pollution from Serving BS}} + \underbrace{N^I \cdot \frac{P^E}{\zeta^\gamma \cdot d_{\text{MAX}}^\gamma \cdot f^\eta \cdot c}}_{\text{RF Pollution from neighbor BSs (UB)}} \quad (4)$$

Although this assumption may appear too conservative at the first glance, as the distance between the current pixel p and each neighbor is in general larger than $\zeta \cdot d_{\text{MAX}}$, in this work we show that the total RF pollution introduced by N^I neighbors does not significantly affect the results, compared to the case in which no RF pollution from the neighbors is assumed.

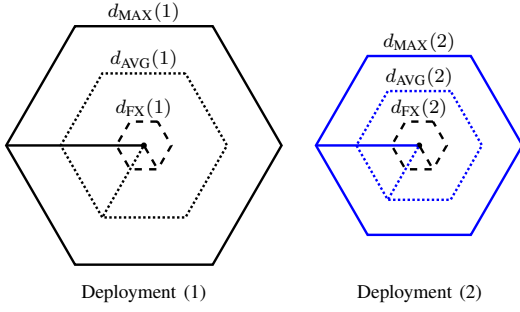


Fig. 2. An example of d_{MAX} , d_{AVG} and d_{FX} in two hexagonal deployments. $d_{\text{MAX}}(2) < d_{\text{MAX}}(1)$, $d_{\text{AVG}}(2) = \alpha \cdot d_{\text{MAX}}(2)$, $d_{\text{AVG}}(1) = \alpha \cdot d_{\text{MAX}}(1)$. Consequently, it holds that $d_{\text{AVG}}(2) < d_{\text{AVG}}(1)$, while $d_{\text{FX}}(2) = d_{\text{FX}}(1)$ (figure best viewed in colors).

Single Deployment RF Pollution. Let us now consider a pixel located at an average distance d_{AVG} from the serving BS. Clearly, it holds that $d_{\text{AVG}} < d_{\text{MAX}}$.¹ By exploiting the right-hand side of Eq. (4), the RF pollution P_{AVG}^R at average distance is expressed as:

$$P_{\text{AVG}}^R = \frac{P^E}{d_{\text{AVG}}^\gamma \cdot f^\eta \cdot c} + N^I \frac{P^E}{\zeta^\gamma \cdot d_{\text{MAX}}^\gamma \cdot f^\eta \cdot c} \quad (5)$$

Fig. 1 reports a graphical sketch of the distances appearing in Eq. 5, by considering an hexagonal layout. Specifically, the central BS is the serving one, while the adjacent BSs are the neighbors. Consequently, $N^I = 6$ in this example. By analyzing in detail the figure, we can note that the RF pollution evaluation of the serving BS is done at distance d_{AVG} while the RF pollution of the neighbors is performed at distance $\zeta \cdot d_{\text{MAX}}$.

Since we adopt a regular shape for the coverage area, the average distance d_{AVG} is expressed as $d_{\text{AVG}} = \alpha \cdot d_{\text{MAX}}$, where $\alpha \in (0, 1)$ is a fixed parameter depending on the chosen coverage layout. Consequently, Eq. (5) can be rewritten as:

$$P_{\text{AVG}}^R = \frac{P^E \cdot [\alpha^{-\gamma} + N^I \cdot \zeta^{-\gamma}]}{d_{\text{MAX}}^\gamma \cdot f^\eta \cdot c} \quad (6)$$

By expressing P^E as in Eq. (2), we can simplify P_{AVG}^R as:

$$P_{\text{AVG}}^R = P_{\text{TH}}^R \cdot [\alpha^{-\gamma} + N^I \cdot \zeta^{-\gamma}] \quad (7)$$

Let us now consider a pixel at a fixed distance d_{FX} from the serving BS. The relationship between d_{FX} and d_{MAX} is expressed as $d_{\text{FX}} = \beta \cdot d_{\text{MAX}}$, where $\beta \in (0, 1)$ is a fixed parameter. By adopting a procedure similar to Eq. (5)-(7), we can formally introduce the RF pollution P_{FX}^R at distance d_{FX} :

$$P_{\text{FX}}^R = P_{\text{TH}}^R \cdot [\beta^{-\gamma} + N^I \cdot \zeta^{-\gamma}] \quad (8)$$

In our scenarios, we will consider values of d_{FX} in proximity to the 5G BSs, since in general people working/living close to the BSs are the ones expressing the highest concerns about RF pollution. However, the same model can be adopted also for distances up to $\zeta \cdot d_{\text{MAX}}$.

Finally, Fig. 2 reports an example of d_{MAX} , d_{AVG} and d_{FX} in two hexagonal deployments, which are labelled as (1) and

(2), respectively. Since $d_{\text{MAX}}(2) < d_{\text{MAX}}(1)$, it is easy to note that $d_{\text{AVG}}(2) < d_{\text{AVG}}(1)$. However, $d_{\text{FX}}(1) = d_{\text{FX}}(2)$.

RF Pollution Comparison among 5G Deployments.

Let us now consider the comparison among two different 5G deployment types, denoted with indexes (1) and (2), respectively. Each deployment type is characterized by a given set of features, e.g., frequency f , propagation exponent γ , minimum power threshold P_{TH}^R , maximum distance d_{MAX} and radiated power P^E . We initially compare the deployments in terms of ratio of emitted powers $P^E(1)$ and $P^E(2)$, which is denoted as $\delta(P^E)$. By adopting Eq. (2) to express $P^E(1)$ and $P^E(2)$, $\delta(P^E)$ becomes equal to:

$$\delta(P^E) = \delta(d_{\text{MAX}})^{\gamma(1)} \cdot d_{\text{MAX}}(2)^{\gamma(1)-\gamma(2)} \cdot \delta(P_{\text{TH}}^R) \cdot \delta(f)^\eta \cdot \delta(c) \quad (9)$$

where $\delta(d_{\text{MAX}}) = \frac{d_{\text{MAX}}(1)}{d_{\text{MAX}}(2)}$, $\delta(P_{\text{TH}}^R) = \frac{P_{\text{TH}}^R(1)}{P_{\text{TH}}^R(2)}$, $\delta(f) = \frac{f(1)}{f(2)}$, $\delta(c) = \frac{c(1)}{c(2)}$. Clearly, when $\delta(P^E) > 1$, the power radiated by deployment (1) is higher than the one of deployment (2). On the other hand, when $\delta(P^E) < 1$, the opposite holds. Finally, when $\delta(P^E) = 1$, there is no variation in the radiated power among the two deployments.

In the following, we compare the two deployments by introducing the RF pollution ratio at average distance, denoted as $\delta(P_{\text{AVG}}^R)$. By adopting Eq. (7), $\delta(P_{\text{AVG}}^R)$ is expressed as:

$$\delta(P_{\text{AVG}}^R) = \delta(P_{\text{TH}}^R) \cdot \frac{\alpha(1)^{-\gamma(1)} + N^I(1) \cdot \zeta^{-\gamma(1)}}{\alpha(2)^{-\gamma(2)} + N^I(2) \cdot \zeta^{-\gamma(2)}} \quad (10)$$

By assuming the same coverage layout in the two deployments, it holds that $\alpha(1) = \alpha(2) = \alpha$. Consequently, Eq. (10) can be rewritten as:

$$\delta(P_{\text{AVG}}^R) = \delta(P_{\text{TH}}^R) \cdot \frac{\alpha^{-\gamma(1)} + N^I(1) \cdot \zeta^{-\gamma(1)}}{\alpha^{-\gamma(2)} + N^I(2) \cdot \zeta^{-\gamma(2)}} \quad (11)$$

Similarly to $\delta(P^E)$, $\delta(P_{\text{AVG}}^R)$ can take values > 1 , < 1 , or $= 1$, depending on which deployment achieves the lowest RF pollution. However, differently from $\delta(P^E)$, $\delta(P_{\text{AVG}}^R)$ is the RF pollution received by a pixel at average distance $d_{\text{AVG}}(1) = \alpha \cdot d_{\text{MAX}}(1)$ in deployment (1) and average distance $d_{\text{AVG}}(2) = \alpha \cdot d_{\text{MAX}}(2)$ in deployment (2). Hence, $d_{\text{AVG}}(1) \neq d_{\text{AVG}}(2)$ if $d_{\text{MAX}}(1) \neq d_{\text{MAX}}(2)$. We believe that the metric $\delta(P_{\text{AVG}}^R)$ is meaningful, as it may be representative for a user living at an average distance in deployment (1) and at an average distance in deployment (2).

Finally, we introduce the RF pollution ratio at fixed distance, denoted as $\delta(P_{\text{FX}}^R)$. By adopting Eq. (8), $\delta(P_{\text{FX}}^R)$ is expressed as:

$$\delta(P_{\text{FX}}^R) = \delta(P_{\text{TH}}^R) \cdot \frac{\beta(1)^{-\gamma(1)} + N^I(1) \cdot \zeta^{-\gamma(1)}}{\beta(2)^{-\gamma(2)} + N^I(2) \cdot \zeta^{-\gamma(2)}} \quad (12)$$

In this case, it is meaningful to compare the deployments at the same distance $d_{\text{FX}}(1) = d_{\text{FX}}(2)$. This setting is representative for a user living at the same distance from the serving BS in both the deployments. Hence, it holds that $\beta(2) = \beta(1) \cdot \delta(d_{\text{MAX}})$. Consequently, Eq. (12) is rewritten as:

$$\delta(P_{\text{FX}}^R) = \frac{\delta(P_{\text{TH}}^R) \cdot [\beta(1)^{-\gamma(1)} + N^I(1) \cdot \zeta^{-\gamma(1)}]}{\beta(1)^{-\gamma(2)} \cdot \delta(d_{\text{MAX}})^{-\gamma(2)} + N^I(2) \cdot \zeta^{-\gamma(2)}} \quad (13)$$

¹For regular deployments, $d_{\text{AVG}} < \zeta \cdot d_{\text{MAX}}$ also holds.

TABLE I
5G SCENARIOS UNDER CONSIDERATION

| Scenario | Features | $\delta(d_{\text{MAX}})$ | $\delta(P_{\text{TH}}^R)$ | $\frac{\gamma(1)}{\gamma(2)}$ | $\delta(f)$ | $\delta(c)$ |
|----------|--|--|---------------------------|---|--|-------------|
| S1 | Light Densification | 2 ($d_{\text{MAX}}(1) = 500$ [m], $d_{\text{MAX}}(2) = 250$ [m]) | 1 | 1 ($\gamma(1) = \gamma(2) = 3$) | 1 ($f_1 = f_2 = 700$ [MHz]) | 1 |
| S2 | Moderate Densification | 5 ($d_{\text{MAX}}(1) = 500$ [m], $d_{\text{MAX}}(2) = 100$ [m]) | 1 | 1.43 ($\gamma(1) = 3, \gamma(2) = 2.1$) | 1 ($f_1 = f_2 = 700$ [MHz]) | 1 |
| S3 | Light Densification, Frequency Change | 2 ($d_{\text{MAX}}(1) = 500$ [m], $d_{\text{MAX}}(2) = 250$ [m]) | 1 | 1 ($\gamma(1) = \gamma(2) = 3$) | 0.19 ($f_1 = 700$ [MHz], $f_2 = 3700$ [MHz]) | 1 |
| S4 | Same Deployment, Service & Frequency Change | 1 ($d_{\text{MAX}}(1) = 500$ [m], $d_{\text{MAX}}(2) = 500$ [m]) | 0.5 | 1 ($\gamma(1) = \gamma(2) = 3$) | 0.19 ($f_1 = 700$ [MHz], $f_2 = 3700$ [MHz]) | 1 |
| S5 | Strong Densification, Service & Frequency Change | 10 ($d_{\text{MAX}}(1) = 500$ [m], $d_{\text{MAX}}(2) = 50$ [m]) | 0.5 | 1.43 ($\gamma(1) = 3, \gamma(2) = 2.1$) | 0.19 ($f_1 = 700$ [MHz], $f_2 = 3700$ [MHz]) | 1 |

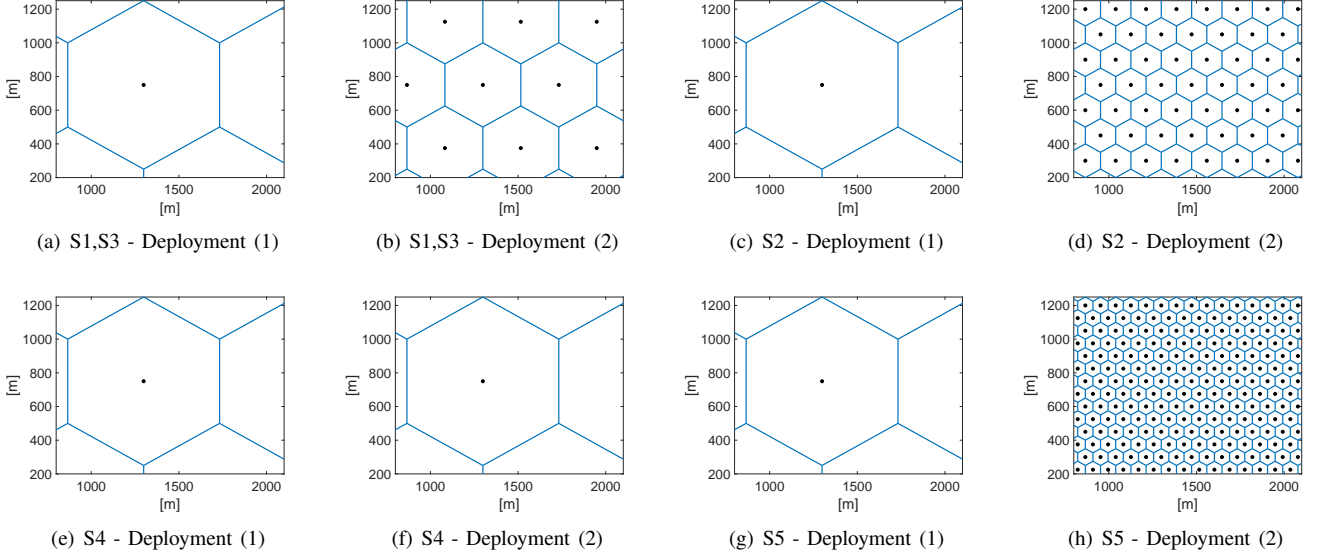


Fig. 3. Visual representation of deployment (1) and deployment (2) across the scenarios S1-S5 (Hexagonal layout).

Similarly to $\delta(P_{\text{AVG}}^R)$, also this metric can take values > 1 , < 1 , or $= 1$. However, differently from $\delta(P_{\text{AVG}}^R)$, the distance between the user and the serving BS is kept constant in the two deployments.

Summarizing, we compare deployment (1) and deployment (2) in terms of emitted power ratio $\delta(P^E)$ (Eq. (9)), RF pollution ratio at average distance $\delta(P_{\text{AVG}}^R)$ (Eq. (11)), and RF pollution ratio at fixed distance $\delta(P_{\text{FX}}^R)$ (Eq. (13)).

III. SCENARIOS

We consider a set of representative scenarios, detailed in Tab. I. Each scenario includes a set of parameters to characterize the pair of deployments under consideration, namely d_{MAX} , P_{TH}^R , γ , f and c . The numerical values for the propagation parameters γ and η are set in accordance to the 5G 3GPP CI propagation model detailed in [9] (3GPP TR 38.901 V14.0.0). By adopting this model, $\gamma = 2.1$ and $\gamma = 3$ for LOS and NLOS conditions, respectively. Moreover, we consider values of $d_{\text{MAX}} \leq 500$ [m]: in this way, as reported by [9], the exponent of the propagation model in LOS conditions does not change with distance. The frequency exponent η is set to 2 for all the scenarios, as in [9]. In addition, we adopt the 5G Italian frequencies in the sub-6 [GHz] spectrum, which is the most promising option for offering coverage and

a mixture of coverage and capacity. Eventually, the baseline path loss c does not vary across the deployments. Actually, this term may be impacted by several factors, like e.g. shadowing [9], but we prefer to keep it constant as it solely appears in the emitted power ratio $\delta(P^E)$, but not in the RF pollution ratios $\delta(P_{\text{AVG}}^R)$ and $\delta(P_{\text{FX}}^R)$. Consequently, $\delta(c) = 1$ in all the scenarios. Finally, each scenario is evaluated over different coverage layouts. More precisely, we consider the following cases:

- Highway layout: the BSs are positioned on a strip, with $\zeta = 1$ to avoid coverage holes;
- Square layout: the BSs are positioned at the intersections of a Manhattan grid, with $\zeta = 1/\sqrt{2}$;
- Hexagonal layout: the BSs are placed on an hexagonal grid, with $\zeta = \sqrt{3}/2$.

Fig. 3 reports a visual representation of the two deployments under consideration in each scenario, for the hexagonal layout. In the following, we provide more details about each scenario:

S1) light densification scenario (Fig.3(a)-3(b)): the only parameter (slightly) changing across deployment (1) and deployment (2) is d_{MAX} . In S1, deployment (2) is lightly denser than deployment (1), while all the other parameters do not vary across the two deployments;

TABLE II
EXPRESSION OF α FOR DIFFERENT COVERAGE LAYOUTS

| Coverage Layout | Closed Formula | Numerical Value |
|-----------------|--|-----------------|
| Highway | $\frac{1}{2}$ | 0.5 |
| Square | $\frac{\sqrt{2}}{6}(\sqrt{2} + \log(1 + \sqrt{2}))$ [11] | 0.5411 |
| Hexagonal | $\left(\frac{1}{3} + \frac{\log 3}{4}\right)$ [11] | 0.6080 |
| Circle | $\frac{2}{3}$ [12] | 0.6667 |

- S2) moderate densification scenario (Fig.3(c)-3(d)), which is subject to a radical variation of d_{MAX} and γ across the two deployments. In S2, the operator adopts a denser deployment in (2) compared to (1). This choice is coupled with a different site deployment strategy and/or site configuration setting, which allow a better coverage over the territory. Consequently, $\gamma(2) < \gamma(1)$;
- S3) light densification plus a frequency change (Fig.3(a)-3(b)). In S3, both d_{MAX} and f are varied in the two deployments. Specifically, while the 700 [MHz] frequency in (1) is primary used to provide coverage, the 3700 [MHz] of (2) allows to achieve a good mixture of coverage and capacity. Moreover, we consider a light reduction of $d_{\text{MAX}}(2)$ compared to $d_{\text{MAX}}(1)$;
- S4) variation of the operating frequency f and of the minimum sensitivity threshold P_{TH}^R (Fig.3(e)-3(f)). In S4, d_{MAX} is not varied, while we assume an increase of P_{TH}^R and f when passing from deployment (1) to deployment (2). With these settings, the operator is able to support a 5G service demanding a higher amount of capacity in deployment (2) compared to (1);
- S5) strong densification scenario (Fig.3(g)-3(h)), in which $d_{\text{MAX}}(2)$ is much lower than $d_{\text{MAX}}(1)$, $P_{\text{TH}}^R(2) > P_{\text{TH}}^R(1)$, $f(2) > f(1)$, and $\gamma(2) < \gamma(1)$. In S5, the operator aims at evaluating the impact of passing from a sparse set of 5G BSs to a very dense deployment. Clearly, this choice has an impact on the propagation conditions, as users in deployment (2) tend to be in LOS conditions w.r.t. the serving 5G BS, resulting in $\gamma(2) < \gamma(1)$. Moreover, the increase of the minimum sensitivity P_{TH}^R and the adoption of an higher frequency f in (2) compared to (1) allows the operator to provide a larger capacity to the users.

We then set the amount of RF pollution N^I generated by the neighboring BSs. To this aim, we consider two distinct cases. In the first one, we assume a perfect coverage provided by the BSs, i.e., each BS radiates power only over the covered area, without polluting the areas covered by other BSs. Consequently, it holds that $N^I(1) = N^I(2) = 0$. In the second case, we assume that each BS radiates power beyond the maximum distance d_{MAX} . In this way, the RF pollution of the current BS is extended to the neighboring areas, which are covered by other BSs. Specifically, we assume an amount of RF pollution equal to the number of adjacent BSs. Therefore, we set $N^I(1) = N^I(2) = 2$, $N^I(1) = N^I(2) = 8$, $N^I(1) = N^I(2) = 6$ for the highway, square, and hexagonal

layouts, respectively.

In the following, we set the values of $\beta(1)$, $\beta(2)$, α across the deployments. Focusing on $\beta(1)$, we initially assume that the RF pollution is evaluated in close proximity to the serving BS in deployment (1). Therefore, we set $\beta(1) = 0.05$ in all the scenarios. Since $d_{\text{FX}} = \beta(1) \cdot d_{\text{MAX}}(1)$, this corresponds in assessing the RF pollution for a user at $d_{\text{FX}} = 25$ [m] from the serving BS. Moreover, we recall that $\beta(2)$ is equal to $\beta(1) \cdot \delta(d_{\text{MAX}})$. Focusing on α , Tab. II reports the closed-form expression and the numerical value for each coverage layout. For the highway layout, $\alpha = 0.5$, as this value corresponds to the average distance in the interval $[0, 1]$ for a BS centered in $x = 0$ with $d_{\text{MAX}} = 1$, i.e., $\alpha = \frac{1}{2} \int_{-1}^1 |x| dx = 1/2$. For the square and hexagonal cases, the average distance is computed as:

$$\alpha = \int_{-\infty}^{+\infty} \int_{-\infty}^{+\infty} f(x, y) \sqrt{x^2 + y^2} dx dy \quad (14)$$

where $f(x, y)$ is the probability density function of a square/hexagon with $d_{\text{MAX}} = 1$ centered in $(0, 0)$. To solve Eq. (14), we adopt the closed-form expressions of average distance retrieved by [11]. We refer the interested reader to [11] for the formal proofs about average distance computation in these two cases. Finally, Tab. II reports as a term of comparison the upper bound of α , which is computed from a circle layout. Interestingly, we can note that the numerical value of α is increasing when passing from the square to the hexagonal layout, but still below the upper bound.

IV. RESULTS

We initially compute the closed-form expressions of RF pollution metrics. We then provide a numerical evaluation to better quantify the impact in terms of RF pollution.

Closed-Form Expressions of RF Pollution Metrics. Tab. III reports the closed-form expressions for $\delta(P^E)$, $\delta(P_{\text{AVG}}^R)$, $\delta(P_{\text{FX}}^R)$ over the different scenarios, by considering the two different neighboring RF pollution options ($N^I = 0$ or $N^I > 0$). The ratio of this step is in fact to provide a ready-to-use tool when considering specific settings for the parameters, e.g., maximum distance increase, frequency increase, propagation conditions change, etc.

Let us first consider the scenarios with $N^I = 0$ (upper part of Tab. III). In the light densification scenario (S1), we vary d_{MAX} across the two deployments. Consequently, $\delta(d_{\text{MAX}})$ is the only term affecting the RF pollution. By recalling that $\delta(d_{\text{MAX}}) > 1$ in S1, we can observe that: i) $\delta(P^E) \gg 1$, ii) $\delta(P_{\text{AVG}}^R)$ does not change across the two deployments, iii) $\delta(P_{\text{FX}}^R) \gg 1$. Consequently, deployment (2) achieves a lower RF pollution than deployment (1) at a fixed distance, i.e., a light densification is able to decrease the RF pollution that is measured at a fixed distance, independently from the chosen coverage layout. Moreover, there is no variation in terms of RF pollution at an average distance from the serving BS.²

²We recall that the fixed distance does not change among deployment (1) and deployment (2), while the average distance is equal to $\alpha \cdot d_{\text{MAX}}(1)$ and $\alpha \cdot d_{\text{MAX}}(2)$ for deployment (1) and deployment (2), respectively.

TABLE III
CLOSED-FORM EXPRESSIONS FOR $\delta(P^E)$, $\delta(P_{\text{AVG}}^R)$, $\delta(P_{\text{FX}}^R)$ IN THE DIFFERENT SCENARIOS AND FOR DIFFERENT VALUES OF N^I .

| $N^I(1) = N^I(2) = 0$ | Scenario | $\delta(P^E)$ | $\delta(P_{\text{AVG}}^R)$ | $\delta(P_{\text{FX}}^R)$ |
|-----------------------|----------|---|---|---|
| | S1 | $\delta(d_{\text{MAX}})^{\gamma(1)}$ | 1 | $\delta(d_{\text{MAX}})^{\gamma(1)}$ |
| | S2 | $\delta(d_{\text{MAX}})^{\gamma(1)} \cdot d_{\text{MAX}}(2)^{\gamma(1)-\gamma(2)}$ | $\alpha^{\gamma(2)-\gamma(1)}$ | $\beta(1)^{\gamma(2)-\gamma(1)} \cdot \delta(d_{\text{MAX}})^{\gamma(2)}$ |
| | S3 | $\delta(d_{\text{MAX}})^{\gamma(1)} \cdot \delta(f)^\eta$ | 1 | $\delta(d_{\text{MAX}})^{\gamma(1)}$ |
| | S4 | $\delta(P_{\text{TH}}^R) \cdot \delta(f)^\eta$ | $\delta(P_{\text{TH}}^R)$ | $\delta(P_{\text{TH}}^R)$ |
| | S5 | $\delta(P_{\text{TH}}^R) \cdot \delta(d_{\text{MAX}})^{\gamma(1)} \cdot d_{\text{MAX}}(2)^{\gamma(1)-\gamma(2)} \cdot \delta(f)^\eta$ | $\alpha^{\gamma(2)-\gamma(1)} \cdot \delta(P_{\text{TH}}^R)$ | $\beta(1)^{\gamma(2)-\gamma(1)} \cdot \delta(d_{\text{MAX}})^{\gamma(2)} \cdot \delta(P_{\text{TH}}^R)$ |
| $N^I(1) = N^I(2) > 0$ | S1 | $\delta(d_{\text{MAX}})^{\gamma(1)}$ | 1 | $\frac{\beta(1)^{-\gamma(1)+N^I(1)} \cdot \zeta^{-\gamma(1)}}{\beta(1)^{-\gamma(1)} \cdot \delta(d_{\text{MAX}})^{-\gamma(1)+N^I(1)} \cdot \zeta^{-\gamma(1)}}$ |
| | S2 | $\delta(d_{\text{MAX}})^{\gamma(1)} \cdot d_{\text{MAX}}(2)^{\gamma(1)-\gamma(2)}$ | $\frac{\alpha^{-\gamma(1)+N^I(1)} \cdot \zeta^{-\gamma(1)}}{\alpha^{-\gamma(2)+N^I(1)} \cdot \zeta^{-\gamma(2)}}$ | $\frac{\beta(1)^{-\gamma(1)+N^I(1)} \cdot \zeta^{-\gamma(1)}}{\beta(1)^{-\gamma(2)} \cdot \delta(d_{\text{MAX}})^{-\gamma(2)+N^I(1)} \cdot \zeta^{-\gamma(2)}}$ |
| | S3 | $\delta(d_{\text{MAX}})^{\gamma(1)} \cdot \delta(f)^\eta$ | 1 | $\frac{\beta(1)^{-\gamma(1)+N^I(1)} \cdot \zeta^{-\gamma(1)}}{\beta(1)^{-\gamma(1)} \cdot \delta(d_{\text{MAX}})^{-\gamma(1)+N^I(1)} \cdot \zeta^{-\gamma(1)}}$ |
| | S4 | $\delta(P_{\text{TH}}^R) \cdot \delta(f)^\eta$ | $\delta(P_{\text{TH}}^R)$ | $\delta(P_{\text{TH}}^R)$ |
| | S5 | $\delta(P_{\text{TH}}^R) \cdot \delta(d_{\text{MAX}})^{\gamma(1)} \cdot d_{\text{MAX}}(2)^{\gamma(1)-\gamma(2)} \cdot \delta(f)^\eta$ | $\delta(P_{\text{TH}}^R) \cdot \frac{\alpha^{-\gamma(1)+N^I(1)} \cdot \zeta^{-\gamma(1)}}{\alpha^{-\gamma(2)+N^I(1)} \cdot \zeta^{-\gamma(2)}}$ | $\frac{\delta(P_{\text{TH}}^R) \cdot [\beta(1)^{-\gamma(1)+N^I(1)} \cdot \zeta^{-\gamma(1)}]}{\beta(1)^{-\gamma(2)} \cdot \delta(d_{\text{MAX}})^{-\gamma(2)+N^I(1)} \cdot \zeta^{-\gamma(2)}}$ |

Eventually, the emitted power in deployment (2) is lower than the one in deployment (1).

Focusing on the moderate densification scenario (S2), both d_{MAX} and γ are varied. Since $\gamma(1) > \gamma(2)$ and $\delta(d_{\text{MAX}}) > 1$, it holds that $\delta(P^E) \gg 1$. Moreover, α appears in the expression of $\delta(P_{\text{AVG}}^R)$ (see Tab. III). By recalling that $\alpha < 1$ (see Tab. II), we can observe that $\delta(P_{\text{AVG}}^R) > 1$. Moreover, it is easy to note that $\delta(P_{\text{FX}}^R) \gg 1$. Therefore, a moderate densification, coupled by an improvement of the channel conditions, is able to notably reduce the RF pollution at the selected locations.

We then move our attention to S3, i.e., the scenario with a light densification and a frequency change. In this case, it is necessary to consider the specific values set to d_{MAX} and f in order to derive the values of $\delta(P^E)$. However, it is interesting to see that both $\delta(P_{\text{AVG}}^R)$, $\delta(P_{\text{FX}}^R)$ do not depend on $\delta(f)$, and they are the same as S1. Consequently, we can conclude that also for S3 the light densification and the frequency change introduce a RF pollution reduction at a fixed distance, and no RF pollution variation at an average distance.

In S4, the main goal is to provide a better service in deployment (2) w.r.t. deployment (1). In this case, the only parameters varied are f and P_{TH}^R , resulting in $\delta(f) < 1$ and $\delta(P_{\text{TH}}^R) < 1$. By inspecting the expression of $\delta(P^E)$ reported in Tab. III, we can clearly see that the emitted power is increased in deployment (2) w.r.t. deployment (1). Moreover, since $\delta(P_{\text{AVG}}^R)$ and $\delta(P_{\text{FX}}^R)$ depends solely on $\delta(P_{\text{TH}}^R)$ in this case, we can conclude that the RF pollution is higher in deployment (2) compared to deployment (1). However, the RF pollution increase can be controlled by properly tuning the minimum threshold ratio $\delta(P_{\text{TH}}^R)$.

Eventually, we consider S5, i.e., the scenario with a strong densification, coupled with a service and frequency change. Since S5 is a mixture of the previous ones, the expressions of $\delta(P^E)$, $\delta(P_{\text{AVG}}^R)$, $\delta(P_{\text{FX}}^R)$ include the terms $\delta(P_{\text{TH}}^R)$ and $\delta(f)$, which in this case are lower than one. As a result, the values of the RF pollution metrics can not be easily inferred in advance, and they have to be numerically evaluated, by considering the

whole set of input parameters.

In the following, we move our attention to the $N^I > 0$ case (bottom part of Tab. III). Clearly, the expression of $\delta(P^E)$ does not change w.r.t. the $N^I = 0$ case, since this term is not affected by N^I .³ Focusing then on $\delta(P_{\text{AVG}}^R)$, a change on the expression only occurs for S2 and S5, i.e., when the path loss exponent varies across the deployments. On the other hand, S1, S3 and S4 are subject to the same expressions of $\delta(P_{\text{AVG}}^R)$ w.r.t. to the $N^I = 0$ case. Therefore, the same comments hold. Finally, we consider $\delta(P_{\text{FX}}^R)$: apart from S4 (which is the same as in the $N^I = 0$ case), all the other scenarios require a numerical evaluation to assess the RF pollution impact.

Numerical Evaluation of RF Pollution. We then solve the expressions in Tab. III by considering the whole set of parameters described in Sec. III, in order to provide the numerical values of RF pollution metrics $\delta(P_{\text{AVG}}^R)$ and $\delta(P_{\text{FX}}^R)$.⁴ Fig. 4 reports the values of $\delta(P_{\text{AVG}}^R)$ and $\delta(P_{\text{FX}}^R)$ over the scenarios S1-S5, the highway/square/hexagonal layouts, and the two options of RF pollution from neighboring BSs (i.e., $N^I = 0$ and $N^I > 0$). Focusing first on $\delta(P_{\text{AVG}}^R)$ and the $N^I = 0$ case (Fig. 4(a)) we can note that the RF pollution ratio is higher than one in scenario S2. Moreover, $\delta(P_{\text{AVG}}^R)$ increases when passing from the hexagonal to the highway layout. This is an expected result, since: i) we have already shown in Tab. III that $\delta(P_{\text{AVG}}^R) = \alpha^{\gamma(2)-\gamma(1)}$, and hence this term is higher than one, ii) we have demonstrated in Tab. II that α is decreased when passing from the hexagonal to the highway layout, (iii) the lower is α , the higher is $\delta(P_{\text{AVG}}^R)$. Focusing on S1 and S3, $\delta(P_{\text{AVG}}^R) = 1$, independently from the coverage layout (as expected). Eventually, $\delta(P_{\text{AVG}}^R) = \delta(P_{\text{TH}}^R) = 0.5$ in S4. Finally, the RF pollution ratio tends to be lower than one in S5, thus showing that deployment (2) pollutes slightly

³The level of RF pollution from neighboring BSs may have also an impact on the level of interference experienced by the pixel. We plan to investigate this issue as a future work.

⁴The numerical values of $\delta(P^E)$ are omitted due to the lack of space.

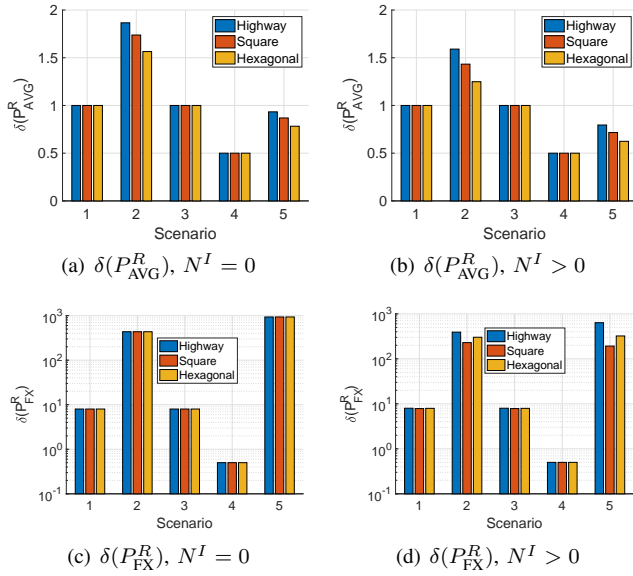


Fig. 4. RF Pollution ratio at average distance $\delta(P_{AVG}^R)$ and at fixed distance $\delta(P_{FX}^R)$ across the different scenarios, for different values of N^I .

more than deployment (1) when the evaluation is done at the average distance.

We then move our attention to $\delta(P_{AVG}^R)$ with $N^I > 0$ (Fig. 4(b)). Interestingly, the RF pollution ratio tends to be decreased in S2 and S5 compared to the $N^I = 0$ case. Moreover, the highway layout always presents a better RF pollution ratio $\delta(P_{AVG}^R)$ compared to the square and hexagonal ones. This result is meaningful, as the RF pollution level coming from neighboring BSs is higher for the square/hexagonal layout compared to the highway one.

In the following, we consider the RF pollution ratio $\delta(P_{FX}^R)$ at fixed distance with $N^I = 0$, shown in Fig. 4(c). Interestingly, $\delta(P_{FX}^R)$ is clearly higher than one in all the scenarios (except from S4). Specifically, the RF pollution ratio at fixed distance is close to 1000 for S5, higher than 400 for S2, and close to 8 for S1 and S3. These scenarios are all subject to a densification of 5G BSs (as $d_{MAX}(2) < d_{MAX}(1)$), which is beneficial for reducing the level of RF pollution at fixed distance. The only scenario with $\delta(P_{FX}^R) < 1$ is S4, which we recall does not include a BS densification, but only a service and a frequency change.

Finally, Fig. 4(d) reports the values of $\delta(P_{FX}^R)$ for the $N^I > 0$ case. As expected, the level of RF pollution coming from the neighboring BSs tends to decrease $\delta(P_{FX}^R)$ in the S2 and S5 scenarios. However, $\delta(P_{FX}^R)$ is always higher than 100 in these scenarios, thus demonstrating that deployment (2) greatly reduces the pollution compared to deployment (1).

V. SUMMARY AND FUTURE WORKS

We have tackled the concern that a proliferation of 5G BSs will result into an uncontrollable RF pollution. To this aim, we have derived a simple - yet effective - model to compare pairs of 5G deployments. Our model takes into account a minimum sensitivity threshold that has to be ensured over the

coverage area, the coverage layout, the RF pollution generated by neighboring BSs, the operating frequency and the channel propagation conditions. The evaluation of RF pollution is done at selected locations, i.e., at a fixed distance from the serving BS or at an average distance, which depends on the chosen coverage layout. We have derived closed form expressions of the emitted power ratio and of the RF pollution ratio at the selected locations. Our results prove that the supposed increase of RF pollution due to the proliferation of 5G BSs is not supported by evidence in most of the considered scenarios. In particular, when the number of BSs is increased (i.e., d_{MAX} is reduced), the level of RF pollution at a fixed distance is decreased of almost three orders of magnitude. Eventually, we have analyzed the conditions which may bring a light increase of RF pollution (e.g., when the number of BSs is not varied and the minimum power threshold is increased). Even in this case, however, the amount of RF pollution can be kept under control. Finally, the RF pollution level from neighboring BSs does not significantly affect the results in most of the scenarios.

We believe that this work can be the first step to a more comprehensive approach, which may evaluate: i) the amount of RF pollution in every location of the territory (and not only at selected locations), ii) the variation of power requirements over space and time (e.g. to match increase/decrease of traffic demands), iii) the adoption of directional antennas, iv) the exploration of frequencies in the mm-Waves bands, v) the impact of irregular coverage layouts.

REFERENCES

- [1] E. Obiedu and M. Giles, "The 5g era: age of boundless connectivity and intelligent automation," *GSM Association*, 2017.
- [2] M.-E. Cousin and M. Siegrist, "The public's knowledge of mobile communication and its influence on base station siting preferences," *Health, Risk & Society*, vol. 12, no. 3, pp. 231–250, 2010.
- [3] *Electromagnetic fields and public health - Base stations and wireless technologies*. Available at <https://www.who.int/peh-emf/publications/facts/fs304/en/>, last accessed on 28th November 2019.
- [4] L. Chiaraviglio, M. Fiore, and E. Rossi, *5G Technology: Which Risks From the Health Perspective?*, pp. 37–48. CNIT, 1 ed., 12 2019. in Marco Ajmone Marsan, Nicola Blefari Melazzi, Stefano Buzzi, Sergio Palazzo, The 5G Italy Book 2019: a Multiperspective View of 5G.
- [5] *A Genève, le gel de nouvelles antennes 5G est confirmé par le Conseil d'Etat (in French)*. Available at <https://tinyurl.com/qt9vqr2>, last accessed on 28th November 2019.
- [6] E. J. Oughton, *et al.*, "An open-source techno-economic assessment framework for 5g deployment," *IEEE Access*, vol. 7, pp. 155930–155940, 2019.
- [7] M. Matalatala, *et al.*, "Multi-objective optimization of massive mimo 5g wireless networks towards power consumption, uplink and downlink exposure," *Applied Sciences*, vol. 9, no. 22, p. 4974, 2019.
- [8] L. Chiaraviglio, *et al.*, "Planning 5g networks under emf constraints: State of the art and vision," *IEEE Access*, vol. 6, pp. 51021–51037, 2018.
- [9] T. S. Rappaport, *et al.*, "Overview of millimeter wave communications for fifth-generation (5g) wireless networks with a focus on propagation models," *IEEE Transactions on Antennas and Propagation*, vol. 65, no. 12, pp. 6213–6230, 2017.
- [10] B. Thors, *et al.*, "Time-averaged realistic maximum power levels for the assessment of radio frequency exposure for 5G radio base stations using massive MIMO," *IEEE Access*, vol. 5, pp. 19711–19719, 2017.
- [11] R. E. Stone, "Some average distance results," *Transportation Science*, vol. 25, no. 1, pp. 83–90, 1991.
- [12] R. C. Larson and A. R. Odoni, *Urban operations research*, pp. 1–573. Prentice Hall, 1 ed., 1981. Englewood Cliffs, NJ.